

Electronic Supplementary Information (ESI) for

Application of transition edge sensor for micro-X-ray fluorescence measurements and micro-X-ray absorption near edge structure spectroscopy: a case study of uranium in biotite obtained from uranium mine

Takumi Yomogida^{*a,b}, Tadashi Hashimoto^c, Takuma Okumura^d, Shinya Yamada^e, Hideyuki Tatsuno^d, Hirofumi Noda^f, Ryota Hayakawa^e, Shinji Okada^g, Sayuri Takatori^h, Tadaaki Isobeⁱ, Takahiro Hiraki^h, Toshiki Sato^j, Yuichi Toyama^g, Yuto Ichinoheⁱ, Oki Sekizawa^k, Kiyofumi Nitta^k, Yuichi Kurihara^l, Shigeru Fukushima^m, Tomoya Uruga^k, Yoshihiro Kitatsuji^a, Yoshio Takahashi^{*b}

^{a.} Nuclear Science and Engineering Center, Japan Atomic Energy Agency, Naka-gun, Ibaraki, 319-1195, Japan, E-mail: yomogida.takumi@jaea.go.jp

^{b.} Department of Earth and Planetary Science, The University of Tokyo, Bunkyo-ku, Tokyo 113-0033, Japan, E-mail: ytakaha@eps.s.u-tokyo.ac.jp

^{c.} Advanced Science Research Center (ASRC), Japan Atomic Energy Agency (JAEA), Naka-gun, Ibaraki, 319-1184, Japan

^{d.} Department of Physics, Tokyo Metropolitan University, Hachioji, Tokyo, 192-0397, Japan

^{e.} Department of Physics, Rikkyo University, Toshima-ku, Tokyo, 171-8501, Japan

^{f.} Department of Earth and Space Science, Osaka University, Toyonaka, Osaka, 560-0043, Japan

^{g.} Engineering Science Laboratory, Chubu University, Kasugai, Aichi, 487-8501, Japan

^{h.} Research Institute for Interdisciplinary Science, Okayama University, Okayama, Okayama, 700-8530, Japan

^{i.} RIKEN Nishina Center, RIKEN, Wako, Saitama, 351-0198, Japan

^{j.} Department of Physics, Meiji University, Kawasaki, Kanagawa, 214-8571, Japan

^{k.} Center for Synchrotron Radiation Research, Japan Synchrotron Radiation Research Institute (JASRI), Sayo, Hyogo, 679-5198, Japan

^{l.} Nagaoka University of Technology, Nagaoka, Niigata, 940-2188, Japan

^{m.} Ningyo-toge Environmental Engineering Center, Japan Atomic Energy Agency, Tomata-gun, Okayama, 708-0601, Japan

Contents

Elemental composition of NIST 610 sample.....	3
Sampling detail of biotite sample.....	4
The XRF spectra fitting.....	5
The XANES spectra of UO₂ measured by SDD and TES	7
References	8

Elemental composition of NIST 610 sample

The elemental composition of the NIST 610 sample is shown in Table S1. The sample was already used in our previous study ¹.

Table S1. Elemental composition of the NIST 610 sample

Element	mg/kg	Element	mg/kg	Element	mg/kg
Antimony(Sb)	415.3	Gold(Au)	25	Selenium(Se)	115.2
Arsenic(As)	340	Iron(Fe)	458	Silver(Ag)	268
Barium(Ba)	453	Lead(Pb)	426	Strontium(Sr)	515.5
Boron(B)	651	Lithium(Li)	488	Thallium(Tl)	61.8
Cadmium(Cd)	244	Manganese(Mn)	457	Thorium(Th)	457.2
Chromium(Cr)	415	Nickel(Ni)	458.7	Titanium(Ti)	437
Cobalt(Co)	390	Potassium(K)	461	Uranium(U)	461.5
Copper(Cu)	444	Rubidium(Rb)	425.7	Zinc(Zn)	433

Sampling detail of biotite sample

Ningyo-toge U mine is located on the border between Okayama and Tottori Prefectures in Japan. The Ningyo-toge U mine is a sandstone-type U deposit. The geology of Ningyo-toge is Mesozoic granite as basement rock. The sedimentary rock layer containing conglomerate, sandstone, and mudstone, namely the Ningyo-toge layer, was formed in the Upper Miocene to Pliocene overlying the weathered granite. The upper part of the granite was weathered. Figure S1 shows a geological columnar section of the core and the appearance of the core samples. The barren ore layer after U extraction was present above the weathered granite layer. The U from the barren ore had likely migrated to the lower layers through groundwater.

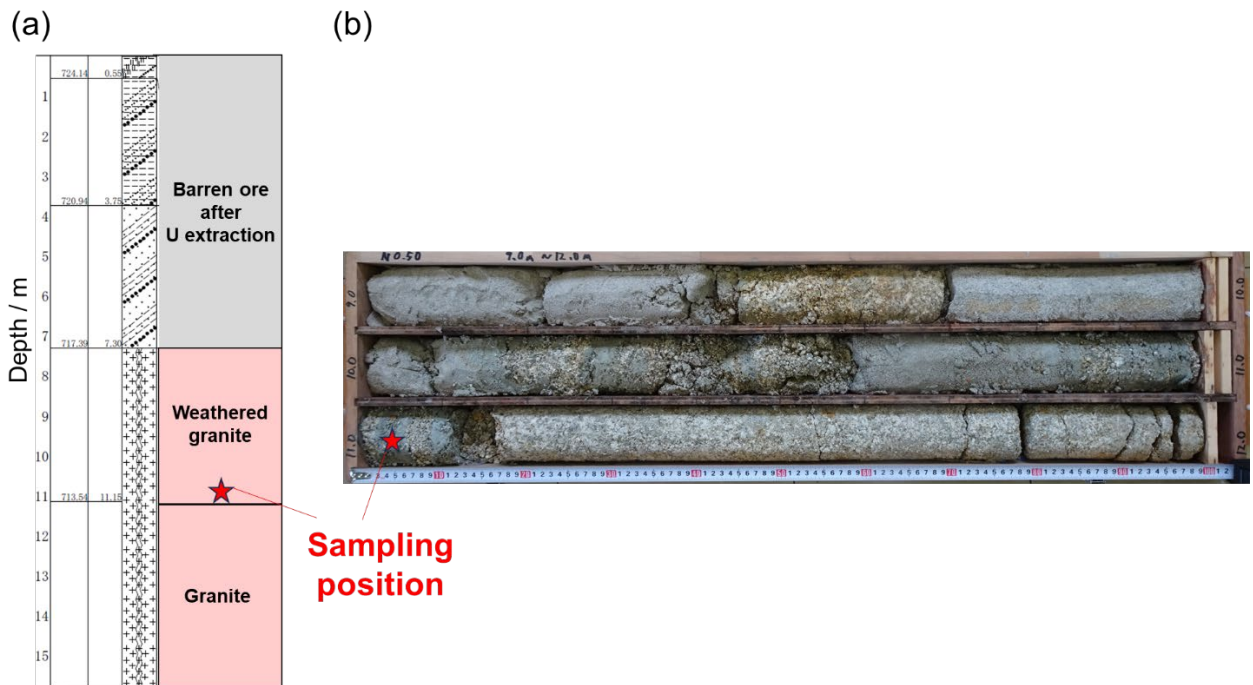


Figure S1. (a) Schematic illustration of boring core. Photographs of the boring core samples of (b) 9.0–12.0 m.

The XRF spectra fitting.

XRF spectra fitting was performed based on the previous report². XRF spectra were fitted by Gaussian peaks. The Rb and U intensities of XRF spectra by SDD were fitted by the two components of the fluorescent X-ray of Rb $K\alpha$ and U $L\alpha$ lines. The Rb and U intensities of XRF spectra by TES were fitted by the three components of the fluorescent X-ray of Rb $K\alpha_1$, Rb $K\alpha_2$ and U $L\alpha$ lines. Rb intensity by TES were calculated by combining the peaks of Rb $K\alpha_1$ and Rb $K\alpha_2$. Figures S2 and S3 show the fitting results of XRF spectra by SDD and by TES, respectively. Table S2 shows the XRF intensities calculated by the Gaussian peak fitting results of XRF spectra. Measured spots are shown in Fig. 4 in the main article.

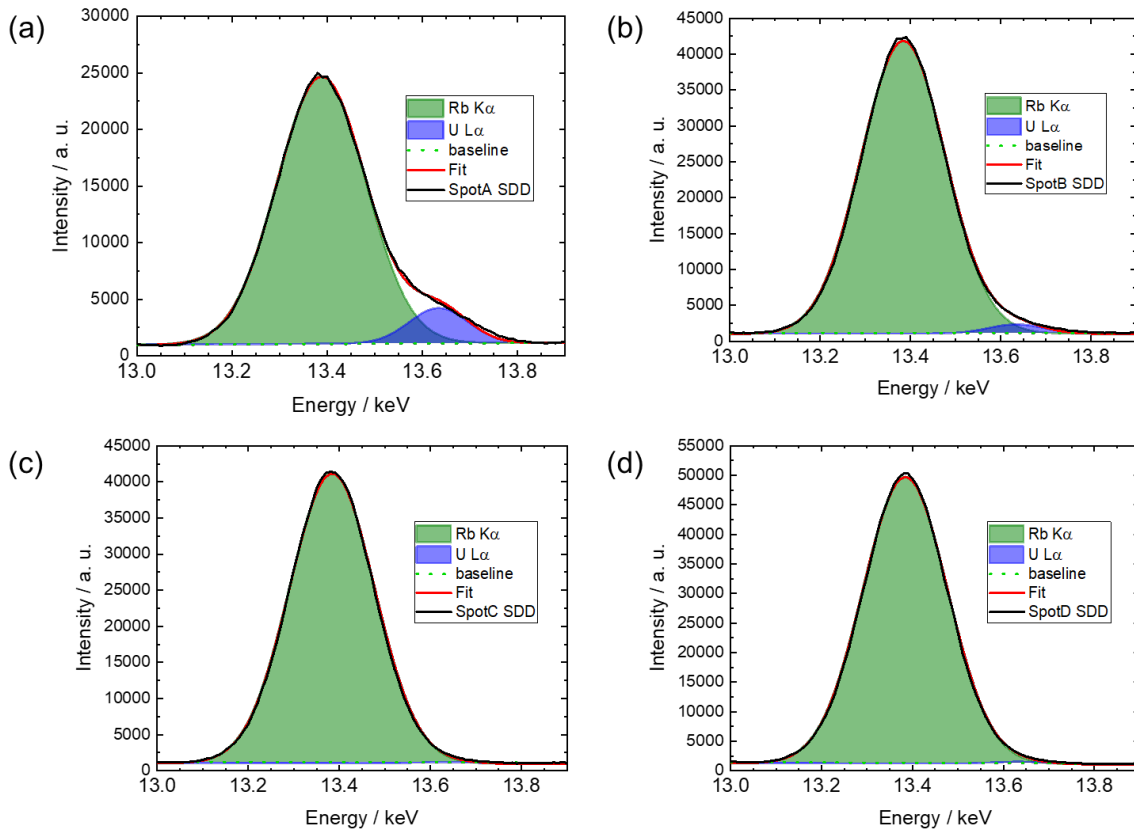


Figure S2. XRF fitting results of the thin biotite sample measured by SDD at spots (a) A, (b) B, (c) C, and (d) D. Measured spots are shown in Fig. 4 in the main article.

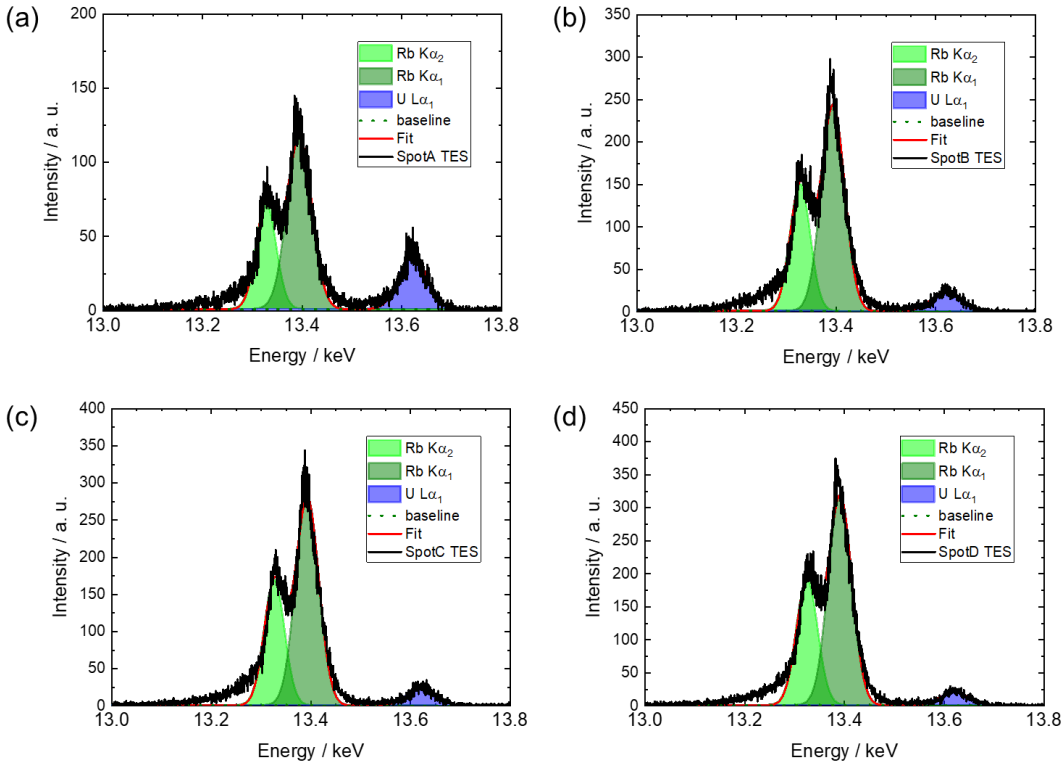


Figure S3. XRF fitting results of the thin biotite sample measured by TES at spots (a) A, (b) B, (c) C, and (d) D. Measured spots are shown in Fig. 4 in the main article.

Table S2. XRF intensities calculated by the Gaussian peak fitting of XRF spectra by SDD and TES.

Measured spots are shown in Fig. 4.

Spot	SDD			TES		
	Rb intensity / counts	U intensity / counts	Rb/U	Rb intensity / counts	U intensity / counts	Rb/U
A	1574079	252655	6.2	10195	2120	4.7
B	2591093	80748	32.1	20869	1385	15.1
C	2550045	9759	261.3	23714	1332	17.8
D	3082884	18205	169.3	27089	1249	21.7

The XANES spectra of UO₂ measured by SDD and TES

UO₂ was used as U(IV) standard samples. The sample was already characterized in our previous study³. The XANES measurements were performed in fluorescence mode by employing an SDD or TES. The XANES spectra at the U L-edge were collected in 0.6 eV steps, with an exposure time of 30 s per step for the sample. The background signals of SDD and TES were 32,000 and 1,000 counts per 30 s, respectively. The sample signals of SDD and TES were 77,4000 and 24,800 per 30 s, respectively.

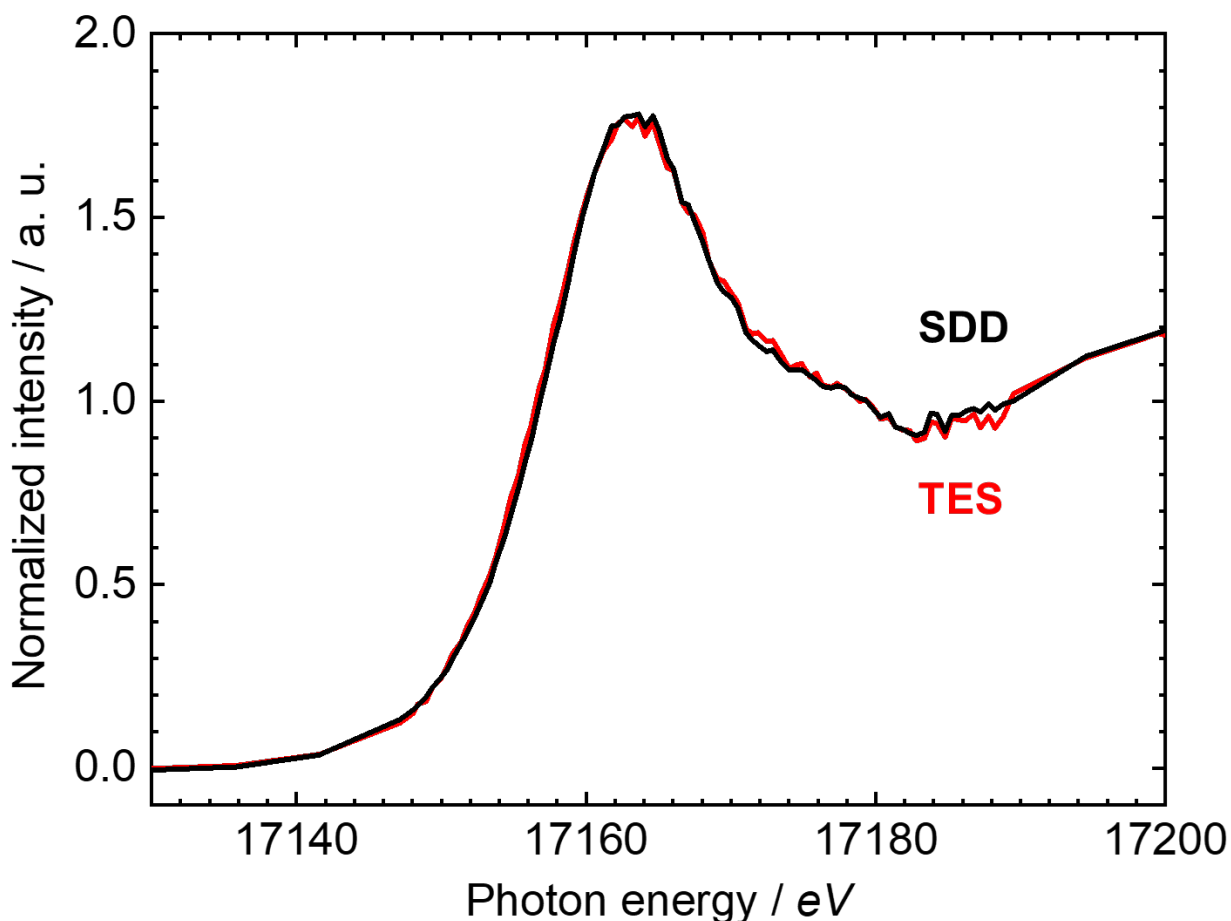


Figure S4. Comparison of the experimental U L₃ edge XANES spectra of UO₂ by SDD (black line) and by TES (red line).

References

- (1) Yamada, S.; Ichinohe, Y.; Tatsuno, H.; Hayakawa, R.; Suda, H.; Ohashi, T.; Ishisaki, Y.; Uruga, T.; Sekizawa, O.; Nitta, K.; et al. Broadband high-energy resolution hard x-ray spectroscopy using transition edge sensors at SPring-8. *Rev. Sci. Instrum.* **2021**, *92* (1), 013103. DOI: 10.1063/5.0020642.
- (2) Yoshii, H.; Takamura, K.; Uwatoko, T.; Takahashi, H.; Sakai, Y.; Screening of uranium contamination on waste surfaces using X-ray fluorescence analysis. *Spectrochim. Acta Part B*, **2022**, *189*, 106368. DOI: 10.1016/j.sab.2022.106368.
- (3) Yomogida, T.; Akiyama, D.; Ouchi, K.; Kumagai, Y.; Higashi, K.; Kitatsuji, Y.; Kirishima, A.; Kawamura, N.; Takahashi, Y. Application of High-Energy-Resolution X-ray Absorption Spectroscopy at the U L3-Edge to Assess the U(V) Electronic Structure in FeUO₄. *Inorg. Chem.* **2022**, *61* (50), 20206-20210. DOI: 10.1021/acs.inorgchem.2c03208.